Analysis and Measurement of Transducer End Radiation in SAW Filters on Strongly Coupling Substrates

A.R. BAGHAI-WADJI, O. MÄNNER, S. SELBERHERR AND F. SEIFERT

Technische Universität Wien
Institut für Allgemeine Elektrotechnik u. Elektronik
Gußhausstraße 27-29 / A-1040 Vienna, Austria

Abstract — **We present the analysis and measurement of spurious responses generated at the ends of interdigital transducers (IDT). Filters fabricated on $LiNbO_3$ show an unwanted pass band ripple whose period indicates additional generation of acoustic waves at the IDT end. As this effect cannot be explained by methods of analysis based on the infinite array approximation, an exact analysis of the complex-valued, frequency-dependent electric charge distribution on the finite IDT structure is required.**
Utilizing the method of moments our analysis is based on a Green's function concept and a spectral domain representation.
Three effects are shown: The first is the charge accumulation on grounded guard fingers located closely to the IDT end, resulting in unwanted end radiation. The second is acoustic end reflections in split-finger IDT's, occurring at the transition from the periodic finger structure to the free substrate. The third is the finger charge induced by the metallic ground plane when the transducer is driven unbalanced to ground. Computer simulations based on our method agree well with measurements.

I. Introduction

Filters fabricated on $LiNbO_3$ show an unwanted passband ripple whose period indicates additional generation of acoustic waves at the interdigital transducer (IDT) end. As this effect cannot be explained by methods of analysis based on the infinite array approximation, an exact analysis of the complex-valued, frequency-dependent electric charge distribution on the finite IDT structure is required [1]. The need for the exact calculation of the charge density distribution is due to the fact that the latter can be regarded as the distributed source for the excitation of acoustic waves in the piezoelectric crystal.
In the following, based on a Green's function concept (for a theortical treatment see for example [2], [3]) , [4], [5], a spectral domain representation [6]-[8], and the method of moments (MoM) [9]-[11], an efficient formalism, [12]-[16] for the calculation of the spatial charge density distribution will be presented. Treating linear boundary value problems, as it is known, the primary task is the construction of Green's function. The latter is the response of the medium under consideration to a Dirac δ−excitation. Generally, the determination of Green's function is a difficult procedure. Using spectral domain representation, the determination of the Green's function in the wave number domain can be simplified considerably. But a problem arises: The resulting Green's function in the wave number domain must be transformed into the real space. This is a difficult procedure, which inherently is accompanied by integral transforms. From a computational point of view, in some cases, it is much easier to transform the product of Green's function and Fourier transformation of the source distribution, which excites the medium. Here, using an exactly calculated expression for the electrostatic part together with an appropriate form for the piezoelectrically excited SAW component of Green's function, the problem of electro-acoustic interaction with arbitrary metallic fingers is solved with analytical formulae. The used Green's function is a good approximation, if the predominant surface acoustic wave is a Rayleigh wave.
First, the associated integral equation is reduced to a matrix equation. Thereby the SAW components of the elements of the involved matrix are evaluated analytically. Then, the resulting matrix is modified in a simple manner, in order to include in the analysis the single and interconnected floating fingers with arbitrary geometrical complexity, [12].
Three effects will be discussed: The first is the charge accumulation on grounded guard fingers located closely to the IDT end, resulting in unwanted end radiation. The second is acoustic end reflections in split-finger IDTs, occuring at the transition from the periodic finger structure to the free substrate. The third is the finger charge induced by the metallic ground plane when the transducer is driven unbalanced to ground.
Several SAW filters consisting of unapodized split-finger IDT's with varying numbers of guard fingers have been fabricated. The frequency response has been measured and transformed into the time domain, where the different effects of interest can be observed separately.
In the final section, results of computer simulations based on our method will be compared with the experimental results. Good agreement could be achieved.

II. Theory

Asumme N infinitely thin metallic strips (fingers) with ideal conductivity deposited on the plane surface of a piezoelectric substrate of finite thickness. The finger geometry and the finger potentials may be arbitrary. The back side of the substrate may be metallized and grounded (Fig.1).

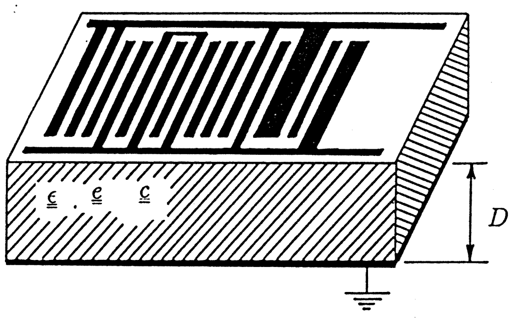

Fig.1 SAW-IDT on a piezoelectric substrate of finite thickness with grounded back plane

The problem is to find an efficient method for the analysis of the frequency-dependent spatial charge density distribution.
The linearity of the boundary value problem sketched in Fig.1 implies the validity of the superposition principle. Equivalent to the latter property is the fact, that the potential on the surface of the substrate, $\Phi(x)$, can be written as a convolution integral

$$\Phi(x) = \int_{-\infty}^{+\infty} G(x'-x)\rho(x')dx', \qquad (1)$$

where $\rho(x)$ is the spatial charge density distribution and $G(x)$ is Green's function characterizing the boundary value problem shown in Fig.1. By definition, $G(x)$ is the potential distribution on the surface of the substrate if a line charge source excites a medium (Fig.2).

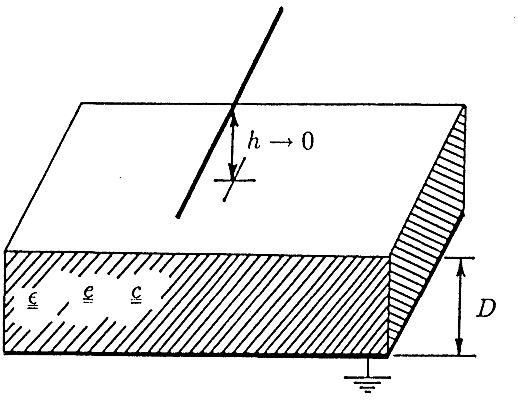

Fig.2 Line charge source excitation of a piezoelectric substrate of finite thickness with grounded back plane

Following the ideas of Milsom et.al. [4], $G(x)$ can be decomposed into two parts

$$G(x) = G^e(x) + G^{saw}(x). \tag{2}$$

$G^e(x)$ and $G^{saw}(x)$, respectively, are the electrostatic and the surface acouctic wave (SAW) components of Green's function. Insertion of (2) in (1) yields

$$\Phi(x) = \Phi^e(x) + \Phi^{saw}(x), \tag{3}$$

with

$$\Phi^e(x) = \int_{-\infty}^{+\infty} G^e(x'-x)\rho(x')dx', \tag{4}$$

and

$$\Phi^{saw}(x) = \int_{-\infty}^{+\infty} G^{saw}(x'-x)\rho(x')dx'. \tag{5}$$

An equivalent formula for $\Phi^e(x)$ is

$$\Phi^e(x) = \frac{1}{2\pi}\int_{-\infty}^{+\infty} \overline{G}^e(k_x)\overline{\rho}(k_x)e^{-jk_x x}dk_x, \tag{6}$$

(Convolution in real space corresponds to the multiplication in the wave number space). The bar indicates Fourier transformation. With regard to Eqs. (5) and (6), and following the concept discribed in [12]-[16], the first step in the solution procedure is to find a reasonabe approximation for $\rho(x)$, and, consequently, for $\overline{\rho}(k_x)$. The second step is to construct appropriate expressions for Green's functions $\overline{G}^e(k_x)$ and $G^{saw}(x)$. Utilizing MoM, in the final step the associated integral equation is reduced to a matrix equation.

III. Approximation of the Charge Density

Asumme that the fingers already have been discretized into NST substrips. Then, with appropriately chosen basis functions $b_l(x)$, the charge distribution on the fingers can be approximated by

$$\rho(x) = \rho_0 \sum_{l=1}^{NST} \rho_l b_l(x). \tag{7}$$

ρ_0 is a normalization factor and ρ_l is the constant unknown charge value on the l^{th} substrip. Employing MoM, most commonly, the impulse, pulse or triangle functions are used as basic functions. The following analysis will be based on pulsfunctions, i.e.

$$b_l(x) = P(x - \xi_l^m, \delta_l), \tag{8}$$

with

$$\Delta_l^b = \int_{-\infty}^{+\infty} b_l(x)dx = x_l^e - x_l^b. \tag{9}$$

Eq.(7) with (8) gives

$$\rho(x) = \rho_0 \sum_{l=1}^{NST} \rho_l \Delta_l^b \frac{1}{\Delta_l^b} P(x - \xi_l^m, \delta_l). \tag{10}$$

Fourier transform of $\rho(x)$ easily can be carried out:

$$\overline{\rho}(k_x) = \rho_0 \sum_{l=1}^{NST} \rho_l \Delta_l^b \frac{1}{\Delta_l^b} \frac{e^{jk_x x_l^e} - e^{jk_x x_l^b}}{jk_x}. \tag{11}$$

In (8), $P(x - \xi_l^m, \delta_l)$ is defined as

$$P(x - \xi_l^m, \delta_l) = \begin{cases} 1, & \text{if } x_l^b \le x \le x_l^e; \\ 0, & \text{otherwise.} \end{cases} \tag{12}$$

The parameters ξ_l^m and δ_l, respectively, are the midpoint coordinate and one half of the width of the l^{th} substrip. x_l^b and x_l^e, respectively, are the start and end point coordinates of the l^{th} substrip.

IV. Green's Function

In this section we will briefly discuss the above mentioned components of Green's function.

IV-1. Electrostatic Component of Green's Function in Wavenumber Domain

In [14] we have shown that $\overline{G}^e(k_x)$ has the functional form

$$\overline{G}^e(k_x) = \frac{1}{\epsilon_0|k_x|}\cdot\frac{1}{1+\epsilon_{P,r}coth(\frac{\epsilon_{P,r}}{\epsilon_{33,r}}D|k_x|)} \tag{13}$$

with

$$\epsilon_{P,r} = \sqrt{\epsilon_{11,r}\epsilon_{33,r} - \epsilon_{13,r}^2}. \tag{14}$$

D is the thickness of the substrate.

Properties of $G^e(k_x)$

i) Behaviour of $\overline{G}^e(k_x)$ for the limit $k_x \to 0$:

$$\lim_{k_x\to 0} \overline{G}^e(k_x) = \frac{D}{\epsilon_0\epsilon_{33,r}} = const. \tag{15}$$

In contrast to Green's function of the semi-infinite substrate, $\overline{G}^e(k_x)$ is regular at point $k_x = 0$. This is because the line charge source, which excites the medium (Fig.2), is not isolated.

ii) Behaviour of $\overline{G}^e(k_x)$ in the limit $D \to \infty$:

$$\lim_{D\to\infty} \overline{G}^e(k_x) = \frac{1}{\epsilon_0(1+\epsilon_{P,r})}\frac{1}{|k_x|}. \tag{16}$$

As it is known, the expression at right hand side is Green's function for a semi-infinite substrshowedate.

IV-2. SAW-Part of Green's Function in Spatial Domain

Milsom et.al., [4], have shown that $\overline{G}^{saw}(k_x)$ can be written as

$$\overline{G}^{saw}(k_x) = \frac{2k_0 G_s}{k_x^2 - k_0^2}. \tag{17}$$

Using Cauchy's residuue theorem they have shown that

$$G^{saw}(x) = -jG_s e^{-jk_0|x|} \tag{18}$$

is valid. G_s is a piezoelectric coupling proportionality. k_0 is the wave number at the free surface of the substrate for a Rayleigh wave propagating with the velocity v_0 at frequency ω.

V. Potential Distribution on the Surface

As we have mentioned above, the potential at the surface can be written as

$$\Phi(x) = \Phi^{e}(x) + \Phi^{saw}(x). \tag{19}$$

At this stage of calculation we have to establish an appropriate innerproduct, denoted by $< u, v >$. In this context, in the theory of MoM, a frequently used innerproduct of two complex-valued functions $u(x)$ and $v(x)$ is defined as

$$< u, v >= \int_{-\infty}^{+\infty} u(x)v^{*}(x)dx. \tag{20}$$

a^{*} is the complex conjugate of a. Next, we have to choose proper weighting functions $w_k(x)$. As in the case of basis functions, usually the impulse, pulse or triangle functions are used as weighting functions. In the present analysis, we will use pulse functions for $w_k(x)$. That is

$$w_k(x) = \begin{cases} 1, & \text{if } x_k^b \le x \le x_k^e; \\ 0, & \text{otherwise.} \end{cases} \tag{21}$$

For a non-equidistant discretization (as in our case), it is necessary to use a modified form of (20) (normalized weighting functions). Appling this, to $\Phi(x)$, we obtain

$$\phi_k = \frac{\int_{-\infty}^{+\infty} \Phi(x) w_k(x)dx}{\int_{-\infty}^{+\infty} w_k(x)dx}, \tag{22}$$

($w_k(x)$ is a real-valued function, therefore we have $w_k^{*}(x) = w_k(x)$). ϕ_k is the applied potential of k^{th} substrip. Inserting (19) in (22) together with

$$\Delta_k^w = \int_{-\infty}^{+\infty} w_k(x)dx = x_k^e - x_k^b, \tag{23}$$

we have

$$\phi_k = \phi_k^e + \phi_k^{saw}, \tag{24}$$

with

$$\phi_k^e = \frac{1}{\Delta_k^w} \int_{-\infty}^{+\infty} \Phi^{e}(x) w_k(x)dx, \tag{25}$$

and

$$\phi_k^{saw} = \frac{1}{\Delta_k^w} \int_{-\infty}^{+\infty} \Phi^{saw}(x) w_k(x)dx. \tag{26}$$

With regard to Eqs. (25) and (26), in the next four calculation steps, we will formulate approximations for $\Phi^{e}(x)$, ϕ_k^e, $\Phi^{saw}(x)$ and finally for ϕ_k^{saw}

V-1. Electrostatic Component of the Potential on the Surface

i) Approximation of $\Phi^{e}(x)$

Insertion of (11) in (6) and subsequent interchange of the order of summation and integration yields

$$\Phi^{e}(x) = \frac{\rho_0}{2\pi} \sum_{l=1}^{NST} \rho_l \Delta_l^b \frac{1}{\Delta_l^b} \int_{-\infty}^{+\infty} \overline{G}^{e}(k_x) \frac{e^{jk_x(x_l^e - x)} - e^{jk_x(x_l^b - x)}}{jk_x} dk_x. \tag{27}$$

ii) Approximation of ϕ_k^e

The insertion of the above equation in (25) and the interchange of the order of summation and integration yield

$$\phi_k^e = \frac{\rho_0}{2\pi} \sum_{l=1}^{NST} \rho_l \Delta_l^b \cdot I_{kl}^e, \tag{28}$$

with

$$I_{kl}^e = \int_{-\infty}^{+\infty} \overline{G}^{e}(k_x) \cdot sinc(\delta_k k_x) \cdot sinc(\delta_l k_x) \cdot e^{-jk_x|\xi_k^m - \xi_l^m|} dk_x. \tag{29}$$

(for $\overline{G}^{e}(k_x)$ see Eqs. (13) and (14)).

Remark

In the limit $D \to \infty$, i.e. a semi-infinite substrate, I_{kl}^e can be calculated analytically

$$\begin{aligned} I_{kl}^e = & \frac{1}{\pi\epsilon_0(1+\epsilon_{P,r})} \cdot \frac{1}{\Delta_k^w \Delta_k^b} \cdot \\ \cdot[+ & (x_k^b - x_l^b)^2 ln|x_k^b - x_l^b| - \\ - & (x_k^b - x_l^e)^2 ln|x_k^b - x_l^e| - (x_k^e - x_l^b)^2 ln|x_k^e - x_l^b| + \\ + & (x_k^e - x_l^e)^2 ln|x_k^e - x_l^e|]. \end{aligned} \tag{30}$$

V-2. SAW Component of the Potential on the Surface

iii) Approximation of $\Phi^{saw}(x)$

Insertion of $\rho(x)$, (10), in (5) and interchange of the order of summation and integration we obtain

$$\Phi^{saw}(x) = -jG_s\rho_0 \sum_{l=1}^{NST} \rho_l \Delta_l^b \frac{1}{\Delta_l^b} I_l(x), \tag{31}$$

with

$$I_l(x) = \begin{cases} \frac{1}{-jk_0}[e^{-jk_0(x_l^e - x)} - e^{-jk_0(x_l^b - x)}], & \text{if } x < x_l^b < x_l^e; \\ \frac{1}{jk_0}[2 - e^{-jk_0(x_l^e - x)} - e^{jk_0(x_l^b - x)}], & \text{if } x_l^b \le x \le x_l^e; \\ \frac{1}{jk_0}[e^{jk_0(x_l^e - x)} - e^{jk_0(x_l^b - x)}], & \text{if } x_l^b < x_l^e < x. \end{cases} \tag{32}$$

iv) Calculation of ϕ_k^{saw}

Insertion of (31) in (26), interchange of the order of summation and integration and performing the associated integrals, we obtain

$$\phi_k^{saw} = -j\rho_0 G_s \sum_{l=1}^{NST} \rho_l \Delta_l^b \cdot \frac{1}{\Delta_k^w \Delta_l^b} I_{kl}^{saw}, \tag{33}$$

with

$$I_{kl}^{saw} = \begin{cases} \Delta_k^w \Delta_l^b sinc(\delta_k k_0) sinc(\delta_l k_0) e^{-jk_0(\xi_k^m - \xi_l^m)}, & \text{if } k \ne l; \\ \frac{2\Delta_l^b}{jk_0}[1 - sinc(\delta_l k_0) e^{-jk_0\delta_l}], & \text{if } k = l. \end{cases} \tag{34}$$

VI. Summary of Relevant Formulae

$$\phi_k = \phi_k^e + \phi_k^{saw}. \tag{35}$$

$$\phi_k^e = \sum_{l=1}^{NST} \rho_l \Delta_l^b \cdot \frac{\rho_0}{2\pi} I_{kl}^e. \tag{36}$$

$$\phi_k^{saw} = \sum_{l=1}^{NST} \rho_l \Delta_l^b \cdot \frac{-j\rho_0 G_s}{\Delta_k^w \Delta_l^b} I_{kl}^{saw}. \qquad (37)$$

with $\frac{\rho_0}{2\pi} = 1$

$$\phi_k = \sum_{l=1}^{NST} \rho_l \Delta_l^b A_{kl}, \qquad (38)$$

where

$$A_{kl} = I_{kl}^e - jG_s \frac{2\pi}{\Delta_k^w \Delta_l^b} I_{kl}^{saw}. \qquad (39)$$

I_{kl}^e and I_{kl}^{saw} as given in (29) and (34).

VII. Experimental Results and Simulations

Three SAW filters $F1$, $F2$ and $F3$, consisting of two unweighted split-finger IDTs were fabricated and measured. The IDTs consisting of 6 active gaps, had a center frequency of 140 MHz and an aperture of 3000 μm. In addition to the active fingers, the filters $F1$, $F2$ and $F3$, respectively, had at left- and right- sides, 0, 6 and 11 dummy fingers The frequency domain measurement was performed with zero fingers grounded. The measurement range was from 45 to 235 MHZ and included the main lobe and the nearest sidelobes of the $sin(x)/x$ transfer function. For a better discrimination of the second order effects involved, the data were transformed into the time domain (Figs. 3, 4 and 5).

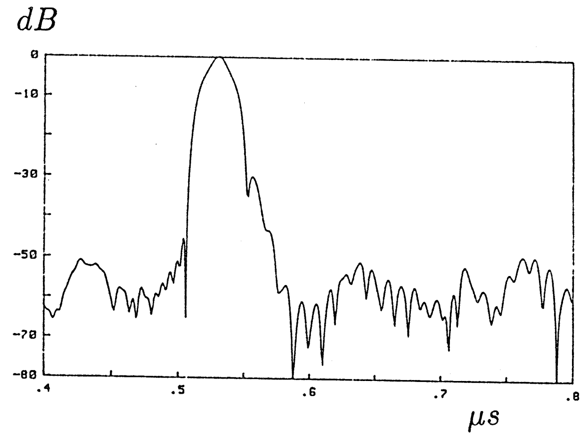

Fig.3 Time domain response of the filter F1

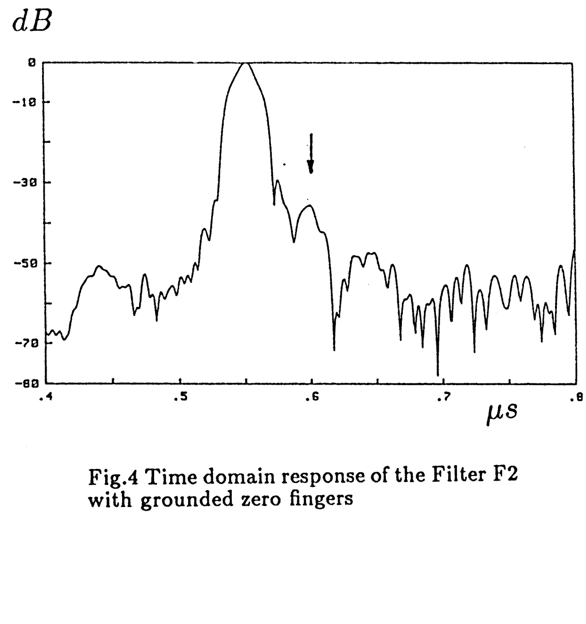

Fig.4 Time domain response of the Filter F2 with grounded zero fingers

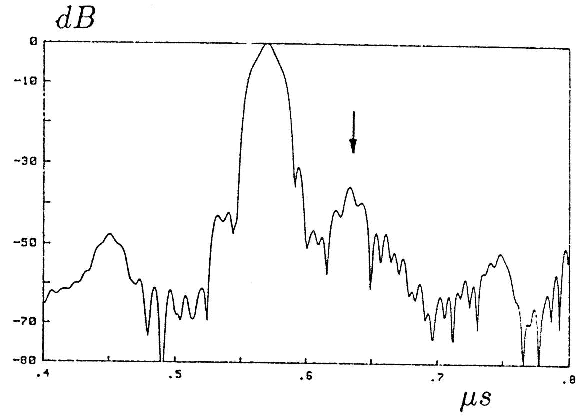

Fig.5 Time domain response of the filter F3 with grounded zero fingers

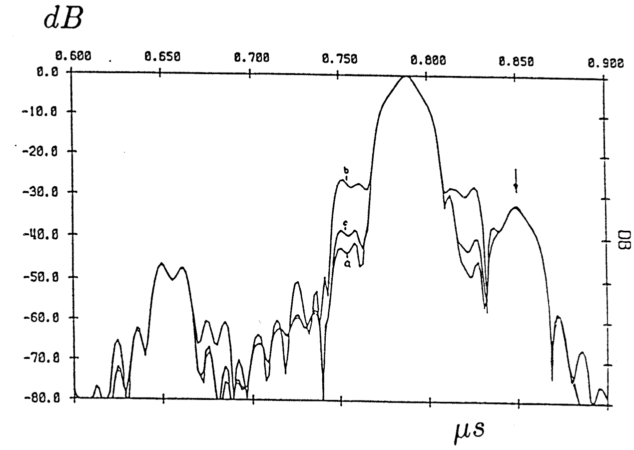

Fig.6 Calculated time domain response of the filter F3. a) grounded zero fingers, b)"hot" zero fingers, c)semi-infinite substrate

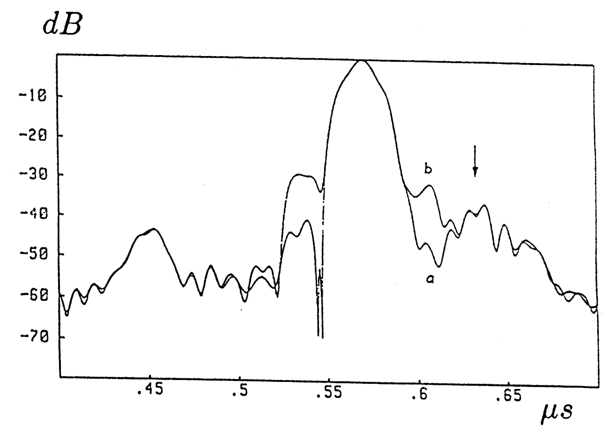

Fig.7 Measured time domain response of the filter F3. a)grounded zero fingers, b)"hot" zero fingers

The trailing peaks marked by arrows in Figs. 4 and 5 result from IDT end reflecitions. While reflecitions cancel within the IDT because of the $\frac{\lambda}{8}$ spaced fingers, this is not the case at the ends.

To demonstrate the versatility of the presented method, we have calculated (Fig.6) the time response of $F3$ for the following two cases: Curve (a) with the zero fingers grounded, and curve (b) with excited zero fingers. For comparison, we have also included the time response of the IDT on a substrate with infinite thickness (curve (c) in Fig.6). The corresponding measurements are shown in Fig.7. The peak appearing before the main response is due to aliasing of the triple-transit signal. The pedestals appering for case (b) at both sides of the main response are due to charge accumulation on the "hot" zero fingers induced by the presence of the grounded backplane. The arrows mark reflections from the IDt ends.

VIII. Conclusion

Employing the method of moments, the concept of Green's function and using the spectral domain representation, an efficient formalism for the analysis of SAW interaction with IDTs has been presented. The influence of the end fingers as well as the infulence of the back plane on the charge distribution have been discussed. Theoretically and experimentally three second order effects in SAW-IDTs are shown. The first is the charge accumulation on grounded guard fingers located closely to the IDT end, resulting in unwanted end radition. The second is acoustic end reflections in split-finger IDTs, occurring at the transition from the periodic finger structure to the free substrate. The third is the finger charge induced by the metallic ground plane when the transducer is driven unbalanced to the ground. Good agreement between computer simulations and experimental results are achieved.

Acknowledgements

This work is supported by Siemens AG, Central Research Laboratories, Munich, West Germany. Partial support by the Austrian Science Research Fund Project 5311 is acknowledged. Special thanks are due to R. Ganss of Siemens AG, Central Research Laboretories, Munich. Valuable comments and helpful discussions with Doz. M. Kowatsch are gratefully appreciated. Continuous encouragement and support by Dr. H Stocker are acknowledged.

References

[1] O. Männer, A.R. Baghai-Wadji, E. Ehrmann-Falkenau and R. Ganss, Mixed nodal variable / scattering parameter formalism for the analysis of SAW transducers, submitted for presentation at European Conference on Circuit Theory and Design, 1987

[2] G.F. Roach, Green's functions, 2nd ed., Cambridge university press, 1967.

[3] R.P. Kanwal, Generalized functions: theory and tequnique, Academic press, mathematics in science and engineering, volume 171, 1983, pp. 217-243.

[4] R.F. Milsom, N.H. Reilly, and M. Redwood, Analysis of generation and detection of surface and bulk acoustic waves by interdigital transducers, IEEE trans. vol. SU-24, No.3, May 1977, pp.147-166

[5] D.P. Morgan, Surface wave devices for signal processing, elsvier, 1985, pp.39-80

[6] T. Itoh, A.S. Herbert, A generalized spectral domain analysis for coupled suspended microstriplines with tuning septums, IEEE trans., vol. MTT-26, No.10, Oct.1978, pp.820-826

[7] T. Itoh, Generalized spectral domain method for multiconductor printed lines and its application to turnable suspended microstrips, IEEE trans., vol. MTT-26, No.12, Dec.1978, pp.983-987

[8] T. Itoh, R. Mittra, A technique for computing dispersion characteristics of shielded microstrip lines, IEEE trans., vol. MTT-22, Oct. 1974, pp.896-898

[9] R.F. Harrington, Field computation by moment method, New York, Mabmillan, 1968.

[10] R.F. Harrington, Matrix methods for fields problems, Proc. IEEE, vol.55, pp-136-149, Feb.1967.

[11] M.M. Ney, Method of moments as applied to electromagnetic problems, IEEE trans. Vol MTT-33, No.10, 1985, pp.972-980.

[12] A.R. Baghai-Wadji, S. Selberherr and F. Seifert, On the calculation of charge, electrostatic poptential and capacitance in generalized finite SAW structures, Proc. IEEE Ultrason. Symp., 1984, pp.44-48.

[13] A.R. Baghai-Wadji, Closed-form formulae analysis of SAW interaction with arbitrary interdigital transducer structures, in Proc. ISSWAS, Novosibirk, 1986

[14] A.R. Baghai-Wadji, S. Selberherr and F. Seifert, A Green's function approach to the electrostatic problem of single, coupled and comb-like metallic structures in anisotropic multilayered media, Proc. AMSE, Sorrento, 1986

[15] ibid, Two-dimensional Green's function of a semi-infinite anisotropic dielectric in the wavenumber

[16] ibid, Rigorous 3D electrostatic field analysis of SAW transducers with closed-form formulae, to be published Proc. UFFC, Williamsburg, VA, 1987